STRUCTURAL BEHAVIOR OF PLAIN AND REINFORCED CONCRETE BEAMS AFFECTED BY COMBINED AAR AND DEF

Renaud-Pierre Martin [1*], Jean-Claude Renaud[1], Stéphane Multon[2], François Toutlemonde[1]

[1]Ifsttar, Université Paris Est, Bridges and Structures Department, Paris, France

[2]Laboratoire Matériaux et Durabilité des Constructions INSA-UPS, Toulouse, France

Abstract

Alkali Aggregate Reaction (AAR) and Delayed Ettringite Formation (DEF) are both internal swelling processes decreasing the mechanical characteristics of the affected concretes. This implies severe concern in terms of serviceability and structural integrity. To check the reliability of the models necessary to manage the structures, their predictions have to be compared to experimental data. In this context, experiments were performed on plain and reinforced concrete beams submitted to a moisture gradient inducing an heterogeneous development of expansions within the structures. Concretes suffering AAR and/or DEF were used. The specimens were monitored in terms of dimensions and water content. After the description of the experimental data, it is checked that the structural behavior of the beams can be interpreted in the frame of the Strength of Materials. Finally, the water content of the beams is correlated with their expansion to emphasize the effect of the reactions on the moisture transfer properties.

Keywords: internal swelling reactions, structural effects, moisture transfer

1 INTRODUCTION

Alkali Aggregate Reaction (AAR) and Delayed Ettringite Formation (DEF) are known to decrease the mechanical properties of concrete. Consequently, the corresponding effects on the structural behavior have to be understood to deal with the affected structures. In particular, to validate the modeling tools necessary to re-assess their serviceability and structural integrity [1,2], it is necessary to compare the numerical predictions to experimental data. In this context, in partnership with EDF (the French power company), extensive laboratory programs have been performed at the French Institute of Science and Technology for Transport and Civil Engineering (Ifsttar, formerly LCPC) concerning AAR [3] and/or DEF [4] to understand in details the field problems indicating that both reactions often act combined: tests were performed on plain and reinforced concrete beams affected by one or both reactions and submitted to moisture gradients. The monitoring of dimensions and water content of these specimens was performed in parallel with the characterization of the expansive properties of the concretes at the scale of the material. All these results provide a database that can be used as a benchmark to validate the numerical tools complementing the investigation purely focused on AAR [5].

This paper illustrates the various effects of AAR and DEF acting separately or combined on the mechanical and hydrous evolution of simple structures such as beams. Firstly, the effect of a moisture gradient is compared to the gradient of expansion imposed to the structure. Then, the strain measurements in the longitudinal direction are compared to the deflection of the beams to check if the structural behavior can

* Correspondence to: renaud-pierre.martin@ifsttar.fr

be interpreted in the frame of the Strength of Materials. Finally, the structural behavior of the beams is correlated to their water content evolution to assess the impact of expansion on the moisture transfers.

2 EXPERIMENTS

2.1 Materials

Three different concrete mixes of various reactivities were used (see Table 1): the mix A is AAR reactive, the mix D is DEF reactive and the mix AD is both AAR and DEF reactive. Each reactivity is obtained by mixing different cements and aggregates and by applying (or not) a heat treatment to the specimens just after casting. The cement C1 (CEM I 52.5) was chosen for the mix A: its high content of alkalis is supposed to trigger AAR (Na_2O_{eq} = 0.92%). To ensure DEF prone conditions, the cement C2 (CEM I 52.5 R) was used because of its high content of aluminates, sulfates and alkalis (respectively 3.46, 4.30 and 0.83 wt. %). The total alkali content of all concretes was increased by adding K_2O in the mixing water respectively up to a value of 1.25 % of the cement content of the mix A and to 1 % for the mixes D and AD. The mix A contains a non-reactive limestone (NRL) sand and reactive limestone (RL) aggregates. Both mixes D and AD contain a non-reactive siliceous (NRS) sand. D contains NRS aggregates. On the contrary, the mix AD contains the same RL aggregates as A. The design of the mixes was carried out with the objective to get similar mechanical characteristics and moisture transfer properties. Previous results [3,6] indicated that, in water, the mix A has an expansive potential of about 0.25% (determined on cylinders of 11 cm in diameter (Ø) and 22 cm in height (H) and on Ø16H32 cylinders) in comparison to the respective 1.51% and 1.50% of the mixes D and AD (determined on Ø11H22 cylinders).

After casting, the concrete A was kept during one week at ambient temperature in its formwork under wet coating to prevent it from drying during setting. The D and AD specimens were submitted to a heat treatment in water just after casting mainly corresponding to a plateau at 81 °C during 72 hours (total duration of the process: one week) [7]. All specimens were then unmolded, sealed under an aluminum-foil cover to prevent them from drying and stored at ambient temperature until the beginning of the tests.

2.2 Test procedure

Specimens and storage conditions

The tests were performed on beams (0.25x0.50x3.00 m^3) as described in Table 2 [4,8]. Some of them were reinforced in the longitudinal direction with two rebars of 32 mm in diameter in the lower part and two rebars of 20 mm in diameter in the upper part; stirrups (12 mm in diameter) are placed every 0.2 m (with a 34 cm-long central zone without stirrups). The concrete cover of the longitudinal rebars is 30 mm for B2 and 42 mm for B4 and B6. The beams were placed on supports (span of 2.8 m with simple bearings) thanks to steel bars embedded at mid-height of the structure. Each specimen was submitted to a moisture gradient during 430 days as described in Figure 1: the lower part of the beam was immersed in water while its upper face is dried in an atmosphere at 30% of Relative Humidity (RH). All lateral sides were sealed with adhesive aluminum foils. The objective of this storage technique was to ensure a vertical moisture gradient [9] to provide an heterogeneous development of the expansive reactions as it occurs in the field. All tests were performed at a constant temperature of 38 °C to speed up the drying process and the swelling reactions.

Dimensions monitoring

The dimensions of the specimens were monitored continuously during the test. In the vertical direction, measurements were made locally at depths (relatively to the upper face) of 0.08 m, 0.17 m, 0.27 m and 0.37 m with embedded vibrating wire sensors (85 mm-long) for the beams B1 and B2. For the beams B3 to B6, measurements were performed at depths of 0.08 and 0.37 m with embedded strain gauges (100 mm).

In the longitudinal direction, the dimensions of the beams were monitored as described in Table 3. Strains were measured locally with small sensors like vibrating wire sensors (85 mm) embedded in the fresh concrete (except from B3) or with embedded strain gauges (100 mm). The global deformations were monitored with vibrating wire sensors or displacement transducers whose lengths are similar to the length of the beams. Finally, the deflection of the specimens at mid span was monitored at mid height with displacement transducers on each side. In this paper, a positive strain corresponds to an extension. Regarding the measurement of deflections, negative values correspond to a bent-down structure.

Water content monitoring

Due to their storage conditions, the beams exchange water with the surrounding atmosphere. The water content global variation of the beams can be monitored by weight survey. A specifically-designed device was used as described in [9]: the load cell consists of a ring-shaped load sensor whose deformation is measured with a vibrating wire sensor; the deformation of the ring is first measured under the (unknown) load of the beam; the load cell is then submitted to the (known) load of a reference steel beam and calibrated masses are afterwards added until the deformation measured reaches the same value as for the tested beam.

3 RESULTS AND DISCUSSION

3.1 Structural behavior of plain beams

Expansion in the vertical direction

Figures 2 to 4 illustrate the vertical strains measured in the beams during the test. They are compared to the free expansion of the materials in water. In the vertical direction, the measured deformation can be considered as an expansion free of restraint: indeed, the water supply conditions of the specimens induce a vertical moisture gradient; as a consequence, the expansion in a given horizontal plane is believed to be homogeneous. Thus, the measurement of the vertical strain can be assimilated to an assessment of the advancement of the swelling reaction while compared to the free expansion.

By applying a moisture gradient, it was aimed to impose a vertical expansion gradient to the specimens. The measurements confirm this: at each timestep, the deeper the measurement, the greater the expansion: the swelling measured is strongly dependent of the amount of water migrating from the immersed lower part or migrating to the drying upper face.

For specimen B1, it can be seen that final expansion nearly reaches the free expansion potential at the end of the 430 days of exposure at 0.37 m. The corresponding rate is however lower. This can be explained by the couplings between AAR expansion and humidity: indeed, the higher the internal humidity, the faster (and greater) the expansion [10,11]; initially, the rate of expansion is determined by the intrinsic water content within the concrete; after the beginning of the test, the internal humidity progressively increases and thus enhances the expansion rate. At the end of the test, the local saturation at this depth is thus probably equal to one, corresponding to this high level of expansion, while the water content history has delayed the development of expansion as compared to a small immersed cylinder.

Similar effects are observed for beams B3 and B5 in comparison with B1, even though, due to the limited range of measurement of the sensors, they could not be monitored until their ultimate expansion. Because of the very high potential of free expansion of the materials D and AD, B3 and B5 even collapsed under dead weight effect only after 330 and 180 days of exposure respectively. The earliest rupture of B5 has been attributed to an initiator effect of AAR on DEF in the specific experimental conditions used in this program [6]: indeed, by consuming part of the alkalis of concrete and inducing microcraking, AAR favored the precipitation of ettringite and thus the development of DEF.

Residual expansion tests

After the rupture of the beams B3 and B5, residual expansion tests were performed to quantify the advancement of the internal swelling reaction as a function of the distance to the lower imbibition area. Cylinders (0.11 m in diameter) were drilled out transversally from the beams. Coring was performed at depths of 0.08 m, 0.17 m, 0.27 m, 0.37 m and 0.44 m. The specimens were stored after drilling in water and monitored in terms of axial strain according to [12]. The corresponding results are displayed in Figure 5.

For B3, the residual expansion at 0.44 m was about 0.16%. This indicates that the rupture occurred before the whole expansion of the material was consumed and thus emphasizes the highly deleterious effects of DEF. On the contrary, the residual expansion at a depth of 0.08 m is 1.90% and indicates that limited expansion has occurred in this area during the test. The expansion measured is even higher than the potential swelling assessed on cylinders free of restraint (1.51%): such an effect has been explained by the existence of microcracks induced by drying that weaken the material and thus enhance the DEF expansion [4].

For B5, the results indicate that the progression of expansion from the lower part was even faster. At a depth of 0.44 m, the whole potential expansion had been consumed. The order of magnitude of the residual expansion at depths of 0.37 m and 0.27 m is lower than 0.09%. Thus, the potential expansion has been nearly fully consumed up to the mid-depth of the cross section. At a depth of 0.08 m, the advancement of the reaction is lower but significant swellings did however occur since the residual expansion reaches only 0.71%.

Mechanical behavior in the longitudinal direction

The global bending behavior of the beams consists in the mechanical response to an imposed deformation profile along its height. Figure 6.a represents the linear regression of all measurements in the longitudinal direction as a function of the corresponding depths for the beam B3. For each timestep, a plane section can be drawn. Due to the high moisture content in the lower part, the imposed expansion in this area is higher than in the upper part and thus leads the beam to bend down (see Figure 6.b). For all other plain concrete beams, the results are similar and are therefore not described here.

The deflection of the beams can be calculated with a double integration of the curvature along the longitudinal axis of the specimen. Due to the symmetry of the water supply conditions, the curvature is believed to remain constant along this axis and, according to the Strength of Materials theory, corresponds to the slope of each line of Figure 6.a. Figure 6.b compares the measured deflection at mid span to this calculation for beam B3. The very good correlation of the two methods confirm the consistency of this approach: the longitudinal structural behavior of the plain beams can thus be fully described with the mean longitudinal strain and the curvature of a plane section.

Figure 7.a illustrates the evolution of the mid-span deflection for the plain concrete beams. The measurements are consistent with the magnitude and the rate of free expansion of the concretes. The deflection of B1 reached a value of about 5 mm while for B3 and B5 it reached up to about 40 mm and 60 mm respectively. For these latter beams, a divergence between the deflections measured on each side of the structure can be noted after 260 and 100 days respectively. This is the consequence of a longitudinal restraint in the u-shaped support (see Figure 1) because of a too high global expansion.

Figure 8 represents the crack patterns of the beams at the end of the test. Since the cracking evolution of B5 and B6 was very similar to that of B3 and B4 respectively, the corresponding results are not presented here. Consistently with the bending of the structures, transverse cracks appeared firstly on the bottom face of the plain beams (see Figures 8.a and c). A map cracking developed later. In the case of B3 (resp. B5), and after the opening of many transverse cracks running from the bottom face to the upper face, one of these cracks opened drastically until the rupture after 330 days (resp. 180 days).

3.2 Structural behavior of reinforced beams

Expansion in the vertical direction

Figures 2 to 4 illustrates the evolution of the vertical strains in the reinforced beams. In each case, the strain overpasses 0.2% in the lower part (depth of 0.37 m) and thus indicates that the stirrups have reached plastic deformations considering steel to concrete bond has remained effective (which is probably true).

While the extent of expansion at 0.37 m remains near 0.2% in B2 (mix A) it reaches a value of about 0.4% for B4 (D) and B6 (AD) respectively at 310 and 230 days. These values have to be compared to the free expansion of the corresponding materials which are respectively 0.25%, 1.51% and 1.50%. Thus, regarding AAR, the vertical expansion is slightly decreased due to the stirrups. A reduction is observed as well for B6 compared to B5 apparently with a much higher extent (no calculation of the reduction could be done since the expansions were not stabilized). This effect seems not so clear for the beam B4 when compared to B3. However this qualitative comparison requires further confirmation taking the reaction rate into account.

Mechanical behavior in the longitudinal direction

Initially, the mechanical behavior of the reinforced beams is similar to the plain ones: the high moisture content in the lower part led the structure to bend down because of the imposed expansions in this area. Figure 6.c illustrates the result of linear regressions of all longitudinal measurements along the height of B4 at different timesteps (results corresponding to B2 and B6 are similar and are therefore not presented here). Once again, the plane sections remain plane during the test. Until 250 days of exposure, the curvature of the section increases. Its integration is fairly consistent with the mid-span deflection as it is illustrated in Figure 6.d. After 250 days, the curvature begins to decrease and is finally reversed while the mean expansion still increases. This observation is consistent with the tendency of the beam to bend up (see Figure 6.d). This phenomenon can be attributed to the longitudinal rebars placed in the lower part: while the imposed expansion increased in the lower part (in terms of swelling on the one hand and of affected height on the other hand), the rebars were progressively subjected to tensile loading. Compressive stresses thus appeared in the lower concrete part (similarly to a prestress effect [13,14]) and led the beam to bend up.

The cracking of the specimens supports this analysis: contrarily to the plain beams, almost no transverse cracks appeared on the lower face owing to the presence of rebars. After the specimens started to bend up, transverse cracks appeared on the upper face (see the dashed lines on Figures 8.e and f for B2 and B4; the map cracking observed on this figures developed during another phase of the test not discussed in this paper). Finally, longitudinal cracks appeared on the bottom face which is consistent with the existence of longitudinal compressive stresses (see Figures 8.b and d).

Once again, the evolution of the deflection is consistent with the expansion of the constitutive materials and the corresponding kinetics (see Figure 7.b): the magnitude and rate of deflection are stronger for B4 and B6 in comparison with B2. Contrarily to the case of AAR [3], the beams (partly or totally) affected by DEF did exhibit a positive deflection corresponding to an upper face in tension after 430 exposure days.

3.3 Correlation between mechanical behavior and water content

Figure 9.a illustrates the evolution of the mass of the beams during the tests. It was previously shown that for the specific AAR cases studied in the present research (typical magnitude of expansion of 0.2-0.3%), all beams have a similar hydrous behavior, whatever the reactivity and the reinforcement considered [15]. On the contrary, for DEF-affected beams (combined with AAR or not), it can be seen that each specimen has a specific water content evolution depending on the constitutive material and on the presence of reinforcement. Contrarily to AAR for which all specimens did exhibit a mass loss (i.e. the water uptake contribution is lower than the drying one), all DEF-affected beams exhibited a large weight gain at the end of

the test. This is the consequence of the strong influence of the expansion on the moisture transfer properties. Indeed, in the case of an expansion free of restraint, it has been shown that the water uptake of the material is directly correlated to the expansion [6] and would correspond to the formation of cracks filled with water [4]. In the case of the beams, this could lead to a faster water ingress in the structure. The results presented in Figure 9.a are consistent with this analysis: the weight gain of reinforced beams is lower than for the plain beams: the presence of rebars partly controls the kinetic of expansion and thus the rate of formation of cracks corresponding to a reduced water uptake.

Figure 9.b illustrates the evolution of the water content of the beams as a function of their mean longitudinal expansion as determined previously with the results presented in Figures 6.a and c. For specimens cast with concrete mixes D and AD, it can be seen that, for a specific reinforcement, a given mean expansion leads to a similar water uptake. Moreover, a given mean expansion leads to a higher water uptake for the reinforced specimens. This could be explained by a higher amount of cracks formed because of the highly restrained deformations in the presence of reinforcement.

Such conclusions cannot be drawn for the AAR-affected specimens. Indeed, no weight gain is measured while the mean longitudinal expansion increases. The lower magnitude of expansion could explain this difference. However, even for significant expansions (e.g. 0.13%, see Figure 9.b), while B3 and B5 exhibit a weight gain of about 2.5 kg, a mass loss of 3 kg is measured for B1. This result emphasizes the need to take into account the effect of strong expansions on the evolution of the moisture transfer properties in the modeling tools. Indeed, cracking inducing higher transfer leads to a faster water ingress which will have a significant effect on the development of expansions because of their coupling with the internal humidity.

4 CONCLUSIONS

To understand the structural effects of AAR and DEF acting separately or combined, tests were performed on beams submitted to a controlled moisture gradient with the final objective to induce a gradient of imposed expansion. By monitoring the dimensions (locally and globally) and the water content of the specimens, it was aimed to provide a database useful to better understand the mechanical effects of these reactions at the scale of a structure and to test the predictions of the numerical tools to assess their reliability.

The analysis of the results has confirmed the existence of a gradient of expansion within the structures. The high imposed deformations in the lower part led the beams to bend down initially. It was shown that the plane sections remained plane during the whole test, whatever the reinforcement. Moreover, by integrating the curvature of the section, it was possible to get a good estimate of the mid span deflection. Thus, it was concluded that the structural behavior of such specimens can be described within the frame of the Strength of Materials.

The presence of reinforcement modified the structural behavior. In particular, for significant expansions developed in the lower part, the mechanical reaction of rebars to the imposed tension led to the development of a compression in this area leading the beams to bend up.

Finally, the weight gain of specimens affected by DEF (combined with AAR or not) has been correlated with the mean longitudinal expansion of the structures. It has thus been shown that a direct correlation exist between these two parameters. This could probably be the consequence of an increase of the moisture transfer properties due to the expansions. Regarding AAR, no such effect had been observed, even for significant expansions corresponding to a weight gain in the case of DEF. This seems to indicate that attention has to be paid concerning the assessment of moisture transfer when developing numerical models. Indeed, because of the high coupling between humidity and AAR or DEF, specific coupling laws between moisture transfer properties and expansion should be developed considering the reaction modeled.

Complementary investigations are currently in progress to quantify the influence of expansions on the transfer properties. The final aim is to establish the corresponding coupling law to implement it in models.

ACKNOWLEDGMENTS

The authors are particularly grateful to the staff of the Structures Laboratory at Ifsttar, particularly F.-X. Barin, C. Bazin, J. Billo, S. Dubroca, M. Estivin and L. Lauvin for their help in the tests. E. Bourdarot, E. Grimal and A. Jeanpierre from EDF are also gratefully acknowledged for their financial support. B. Godart and L. Divet are finally thanked for having initiated and directed researches about internal swelling reactions at Ifsttar for more than 15 years.

5 REFERENCES

[1] Sellier, A., Bourdarot, E., Multon, S., Cyr, M., Grimal, E. (2009): Combination of structural monitoring and laboratory tests for assessment of alkali-aggregate swelling: application to gate structure dam. ACI Materials Journal (106-3): 281-290.

[2] Seignol, J.-F., Baghdadi, N., Toutlemonde, F. (2009): A macroscopic chemo-mechanical model aimed at re-assessment of d affected concrete structures. 1st international conference on computational technologies in concrete structures, May 24 – 27, 2009, Korea: 422-440.

[3] Multon, S. (2004): Evaluation expérimentale et théorique des effets mécaniques de l'alcali-reaction sur des structures modèles. ERLPC (OA 46), Laboratoire Central des Ponts et Chaussées: pp 423.

[4] Martin, R.-P. (2010): Experimental analysis of the mechanical effects of delayed ettringite formation on concrete structures (in French), PhD thesis, Université Paris Est: pp 577.

[5] Toutlemonde, F., Multon, S., Seignol, J.-F. (2004): Extensive data basis for validating ASR models: a French contribution to the re-assessment of ASR-affected structures. 12th international conference on alkali-aggregate reaction, October 15 – 19, 2004, Beijing, China: 31-40.

[6] Martin, R.-P., Renaud, J.-C., Toutlemonde, F. (2010): Experimental investigations concerning combined delayed ettringite formation and alkali-aggregate reaction. 6th international conference on concrete under severe conditions, June 7 – June 9, 2010, Merida, Mexico: 287-295.

[7] Martin, R.-P., Toutlemonde, F. (2010): Design of a heat treatment representative of the curing conditions of a massive concrete structure. Bulletin de Liaison des Ponts et Chaussées (278): 49-63.

[8] Multon, S., Toutlemonde, F. (2010): Effect of moisture conditions and transfers on alkali silica reaction damaged structures. Cement and Concrete Research (40): 924-934.

[9] Multon, S., Merliot, E., Joly, M., Toutlemonde, F. (2004): Water distribution in beams damaged by ASR: global weighing and local gamadensitometry. Materials and Structures (40): 282-288.

[10] Larive, C. (1998): Apports combinés de l'expérimentation et de la modélisation à la compréhension de l'alcali-réaction et de ses effets mécaniques. ERLPC (OA 28), Laboratoire Central des Ponts et Chaussées: pp 404.

[11] Poyet, S., Sellier, A., Capra, B., Thévenin-Foray, G., Torrenti, J.-M., Tournier-Cognon, H., Bourdarot, E. (2006): Influence of water on alkali-silica reaction: experimental study and numerical simulations. Journal of Materials in Civil Engineering (18-4): 588-596.

[12] Pavoine, A., Divet, L. (2009): Réaction Sulfatique Interne au béton – Essai d'expansion résiduelle sur carotte extraite de l'ouvrage, Méthode d'essai des Laboratoires des Ponts et Chaussées (ME 67), Laboratoire Central des Ponts et Chaussées: pp 28.

[13] Koyanagi, W., Rokugo, K., Ishida, H. (1986): Failure behaviour of reinforced concrete beams deteriorated by Alkali-Silica Reactions. 7th international conference on alkali-aggregate reaction, 1986, Ottawa, Canada: 141-145.

[14] Monette, L.J., Gardner, N.J., Grattan-Bellew, P.E. (2002): Residual strength of reinforced concrete beams damaged by alkali-silica reaction – Examination of damage rating index method. ACI Materials Journal (99): 42-50.

[15] Multon, S., Toutlemonde, F. (2004): Water distribution in concrete beams. Materials and Structures (37): 378-386.

TABLE 1: Concrete mixes (kg/m³).
* NRL=Non Reactive Limestone; NRS=Non Reactive Siliceous aggregate; ARL=Alkali Reactive Limestone; d_{min}/d_{max}=minimal and maximal particle size (mm)

Mix	Reactivity	Cement type	Cement	Water	NRL*	NRS*			ARL*				Na_2O_{eq}
					0/5	0/2	4/8	8/12	4/7	7/10	10/14	14/20	
A	AAR	C1	410	205	621	-	-	-	175	92	319	536	1.25%
D	DEF	C2	410	188	-	854	100	829	-	-	-	-	1%
AD	AAR+DEF	C2	410	188	-	797	-	-	114	29	843	-	1%

TABLE 2: Beam specimens (P = Plain; R = Reinforced)

	B1	B2	B3	B4	B5	B6
Mix	A	A	D	D	AD	AD
Reinforcement	P	R	P	R	P	R

TABLE 3: Sensors placed in the vertical direction (S = Sensor; ML = Measurement Length (mm); VW = Vibrating Wire; SG = Strain Gauge; DT = Displacement Transducer).

	B1		B2		B3		B4		B5		B6	
Depth (m)	S	ML	S	ML	S	ML	S	ML	S	ML	S	ML
0.03	VW	2980	VW	2980	DT	2980	DT	2980	DT	2980	DT	2980
0.08	VW	85	-	-	SG; VW	100; 85	SG	100	SG	100	SG	100
0.17	VW	85	-	-	SG; VW	100; 85	SG	100	SG	100	SG	100
0.23	VW	2640	VW	2640	DT; VW	2640	DT	2640	DT	2640	DT	2640
0.27	VW	85	-	-	SG; VW	100; 85	SG	100	SG	100	SG	100
0.37	VW	85	-	-	SG; VW	100; 85	SG	100	SG	100	SG	100
0.47	VW	2980	-	-	DT	2980	DT	2980	DT	2980	DT	2980

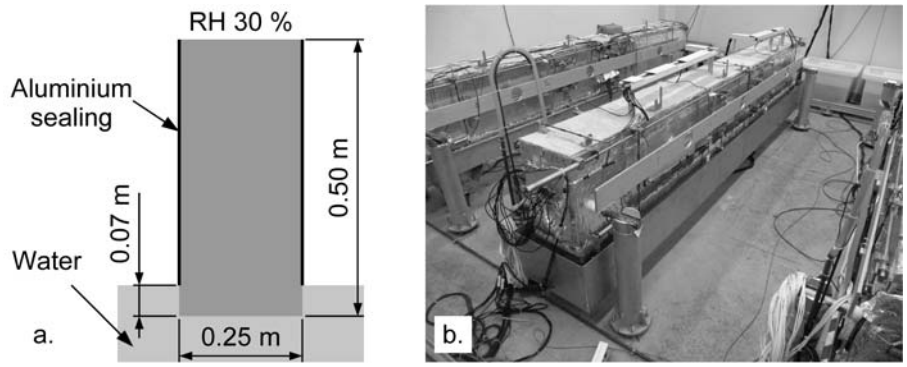

FIGURE 1: Water supply conditions during the test (a. cross section; b. general view).

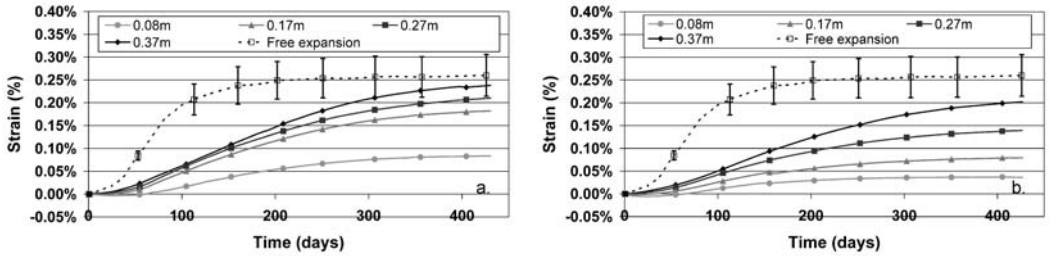

FIGURE 2: Vertical strain in the beams made of concrete A at different depths (a. B1; b. B2).

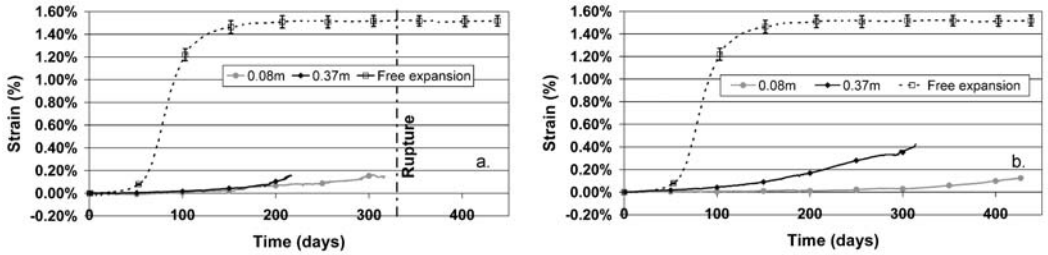

FIGURE 3: Vertical strain in the beams made of concrete D at different depths (a. B3; b. B4).

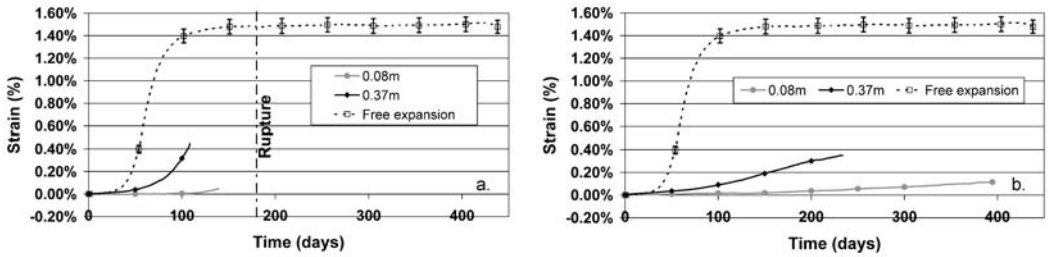

FIGURE 4: Vertical strain in the beams made of concrete AD at different depths (a. B5; b. B6).

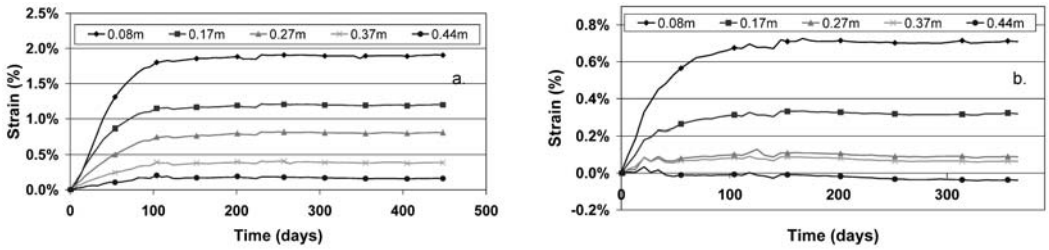

FIGURE 5: Residual expansion at various depths after failure of the beams B3 (a) and B5 (b).

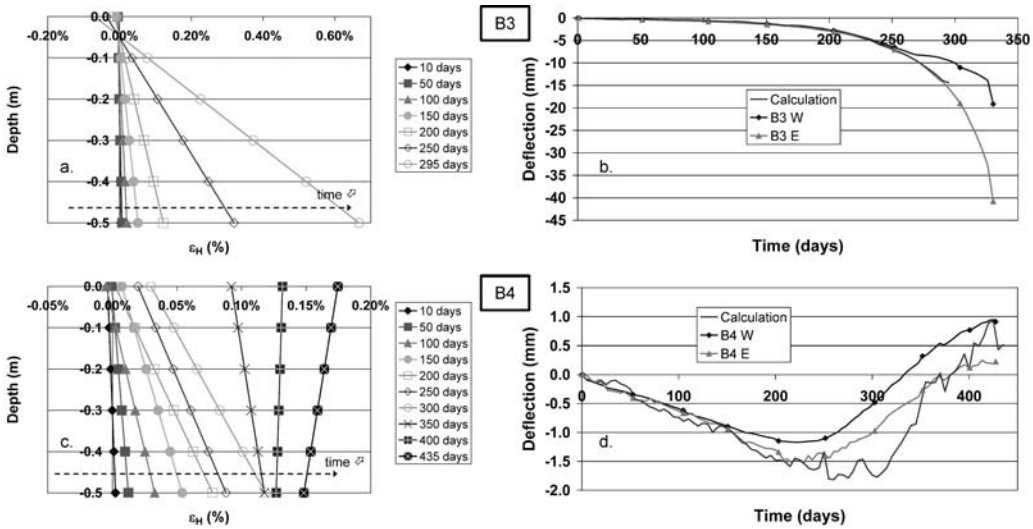

FIGURE 6: Mean longitudinal strain profiles (a and c) and comparison between the integration of their slopes and the deflection measured at mid span (b and d – W = West; E = East) for plain and reinforced beams affected by DEF (respectively B3 and B4).

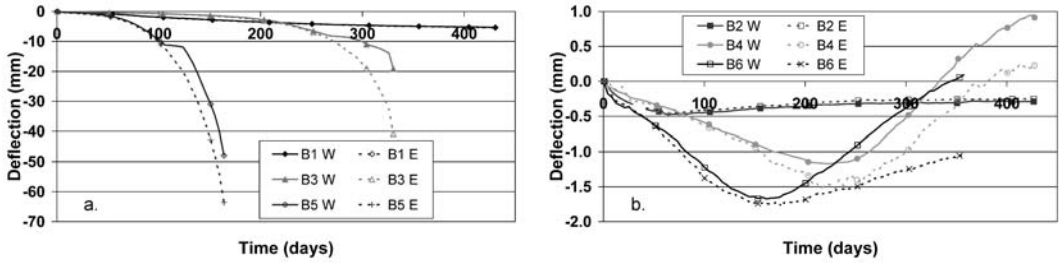

FIGURE 7: Mid span deflection of plain (a) and reinforced (b) beams (W = West; E = East).

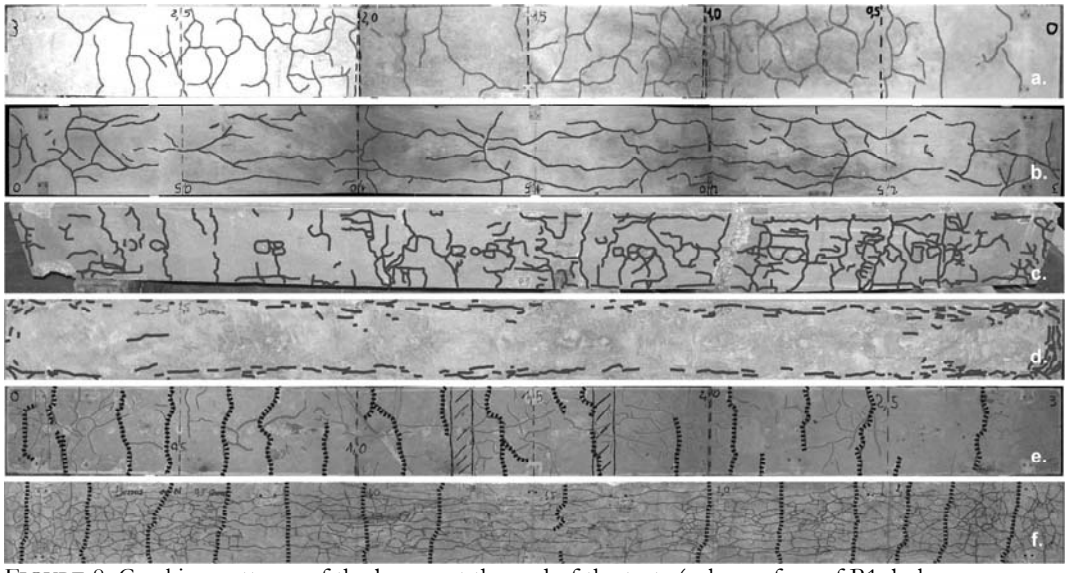

FIGURE 8: Cracking patterns of the beams at the end of the tests (a. lower face of B1, b. lower face of B2, c. lower face of B3, d. lower face of B4, e., upper face of B2, f. upper face of B4 – Map cracking on figures e and f corresponds to tests not described in this paper).

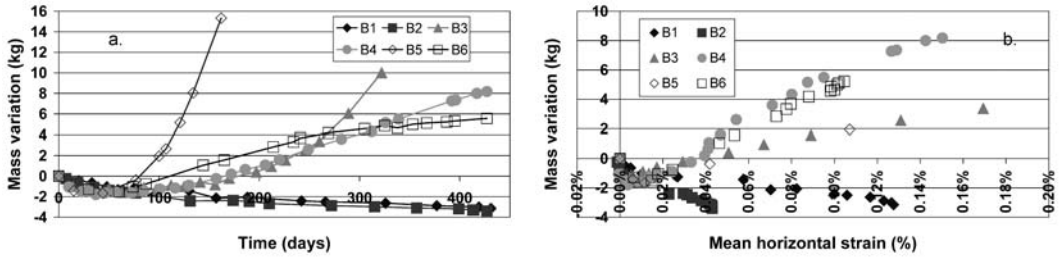

FIGURE 9: Global mass variation of the beams a. vs. time b. correlated to the mean longitudinal expansion.